

Long-Term Creep Rates on the Hayward Fault: Evidence for Controls on the Size and Frequency of Large Earthquakes

by James J. Lienkaemper, Forrest S. McFarland, Robert W. Simpson, Roger G. Bilham, David A. Ponce, John J. Boatwright, and S. John Caskey

Abstract The Hayward fault (HF) in California exhibits large (M_w 6.5–7.1) earthquakes with short recurrence times (161 ± 65 yr), probably kept short by a 26%–78% aseismic release rate (including postseismic). Its interseismic release rate varies locally over time, as we infer from many decades of surface creep data. Earliest estimates of creep rate, primarily from infrequent surveys of offset cultural features, revealed distinct spatial variation in rates along the fault, but no detectable temporal variation. Since the 1989 M_w 6.9 Loma Prieta earthquake (LPE), monitoring on 32 alignment arrays and 5 creepmeters has greatly improved the spatial and temporal resolution of creep rate. We now identify significant temporal variations, mostly associated with local and regional earthquakes. The largest rate change was a 6-yr cessation of creep along a 5-km length near the south end of the HF, attributed to a regional stress drop from the LPE, ending in 1996 with a 2-cm creep event. North of there near Union City starting in 1991, rates apparently increased by 25% above pre-LPE levels on a 16-km-long reach of the fault. Near Oakland in 2007 an M_w 4.2 earthquake initiated a 1–2 cm creep event extending 10–15 km along the fault. Using new better-constrained long-term creep rates, we updated earlier estimates of depth to locking along the HF. The locking depths outline a single, ~50-km-long locked or retarded patch with the potential for an $M_w \sim 6.8$ event equaling the 1868 HF earthquake. We propose that this inferred patch regulates the size and frequency of large earthquakes on HF.

Online Material: 2007 event creep models, plots of creepmeter data, maps and cross-sections of relocated microearthquakes and active fault traces, and iterative solutions for depth of creep.

Introduction

The Hayward fault (HF), a major branch of California's San Andreas fault system, produced an $M \sim 6.8$ earthquake in 1868 (Lawson, 1908; Bakun, 1999). Its paleoearthquake record suggests such events occur regularly and frequently, with a $161 \pm 65(1\sigma)$ and ± 10 yr (± 1 standard error of the mean) mean recurrence interval (Lienkaemper *et al.*, 2010). Given an elapsed time of 143 yr since the last major earthquake in 1868, the 30-yr probability of future large events is calculated to be ~29% ($\pm 6\%$), based on a 1900-yr earthquake chronology (Lienkaemper *et al.*, 2010). Since the 1960s, it has been known that some of the movement of the Hayward fault is relieved aseismically by fault creep over a distance of at least 69 km and probably over the entire fault (~96 km; Lienkaemper *et al.*, 1991). If no aseismic release were occurring, full rupture of the Hayward fault could produce an M 7.2 earthquake every 240 yr (for a loading rate of 9 mm/yr and 2.2 m average slip; Lienkaemper and Borchardt, 1996; Wesnousky, 2008). Thus, the aseismic release

(including both interseismic and postseismic) appears to reduce both the magnitude and recurrence time of expected large earthquakes. Exploring how this aseismic release may occur at depth along the fault, both temporally and spatially, and how any variations in rate might affect its current seismic potential, is the subject of this report.

Earliest estimates of creep rate (Cluff and Steinbrugge, 1966; Blanchard and Laverty, 1966; Bonilla, 1966; Radbruch and Lennert, 1966; Nason, 1971) were based on offset cultural features, and many were multidecadal averages with considerable uncertainty. In the 1970s and 1980s many more creep observations became available, both from additional cultural features and from geodetic surveys, including alignment arrays. Comparisons of the geodetic data to the older multidecadal rates from cultural features suggested some systematic spatial variations, but significant temporal variations were not yet detectable within the uncertainties (Prescott and

Lisowski, 1983; Schulz, 1989; Lienkaemper *et al.*, 1991; Lienkaemper and Galehouse, 1997).

However, on 17 October 1989, the M_w 6.9 Loma Prieta earthquake (LPE) occurred on a dextral-reverse oblique splay of the San Andreas fault in the Santa Cruz Mountains and profoundly changed surface creep rates on the southern Hayward fault, apparently in response to a drop in static stress (~ 0.1 MPa; Lienkaemper *et al.*, 1997, 2001). Immediately following the LPE, we added several new alignment arrays

for a total of over 30, which have now been monitored at least annually for about 20 years (Fig. 1; McFarland *et al.*, 2009). Five satellite-telemetered creepmeters added in the early 1990s have greatly enhanced temporal resolution (Bilham *et al.*, 2004; see Figs. S2–S6 in the electronic supplement to this paper).

In this paper, we summarize significant changes in creep rate along the HF in the past two decades. We describe locations in terms of distances along HF in kilometers

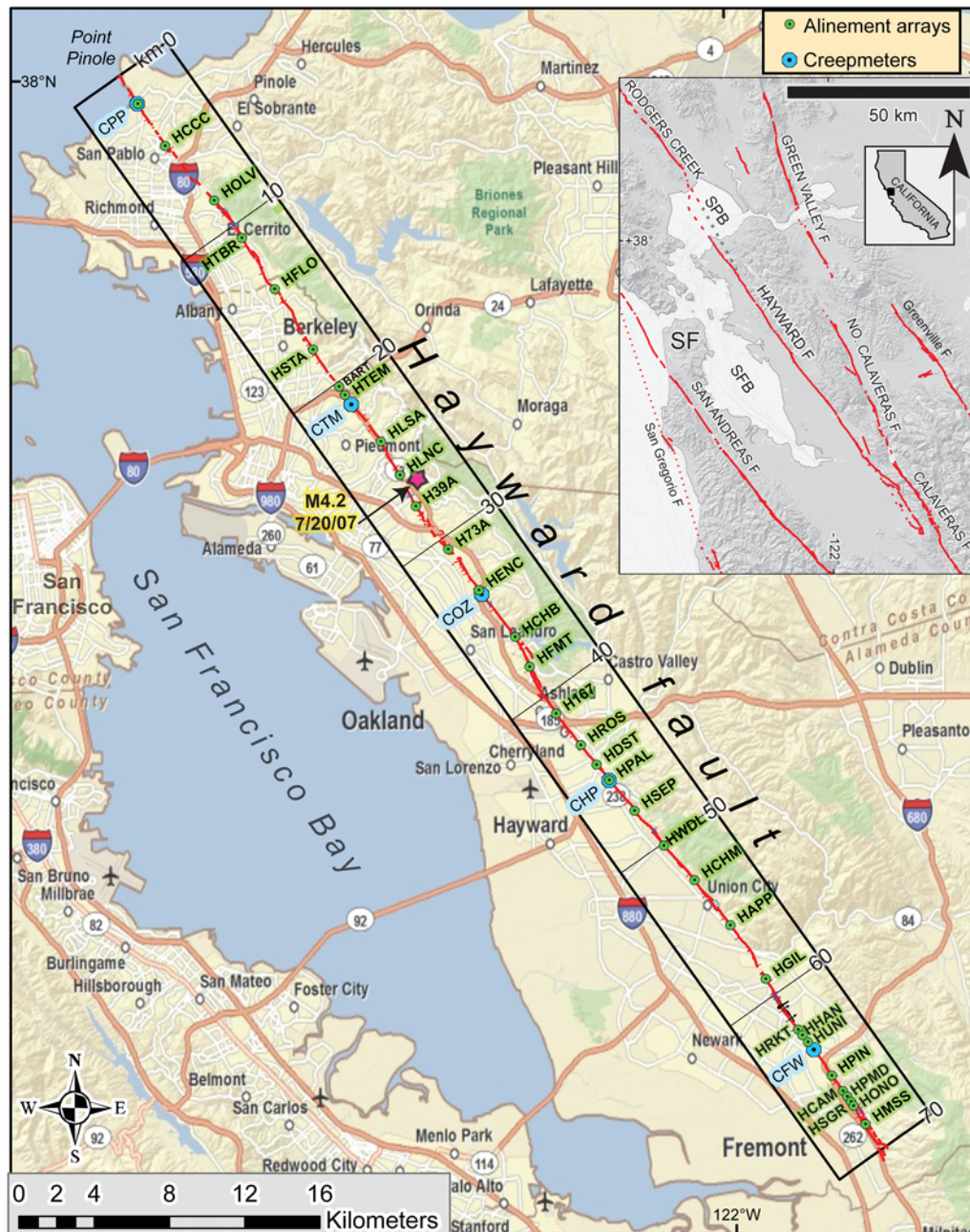


Figure 1. Locations of alignment arrays (in green) and creepmeters (in blue) along the Hayward fault. Grid along fault indicates distance in kilometers from Point Pinole (Lienkaemper, 2006). Star (in magenta) at kilometer 26.43 indicates the epicenter of the M 4.2 (20 July 2007) earthquake associated with a slip transient between arrays HTEM to H73A. Inset map shows other active traces of faults in the San Francisco Bay area (USGS and CGS, 2006); Hayward–Rodgers Creek fault below SPB (from Appendix D in the electronic supplement to this paper). SF, San Francisco; SFB, San Francisco Bay; SPB, San Pablo Bay.

southeastward of Point Pinole (Fig. 1) as defined in Lienkaemper (1992, 2006). These changes in HF creep rate have implications for understanding how creep is released in the near surface and at depth. Temporal changes may reflect the changes in the extent and behavior of the creeping patches and their possible interactions with the locked areas. Taken together these rate changes require an update of the Simpson *et al.* (2001) estimate of HF depth to locking, and we consequently derive new estimates of the seismic potential of the fault based on time elapsed since the 1868 earthquake.

First, we present an overview of the spatial variation of creep rates along the fault, including how well rates have been constrained spatially and temporarily. Then we describe and summarize each of the most significant perturbations to the pre-LPE creep rates and the possible impact of these perturbations on long-term rates. Finally, we use the new average best available long-term rates to update the Simpson *et al.* (2001) calculation of variations in creep rates with depth to locking and summarize the current seismic potential of the fault inferred from the location and extent of locked patches in this model.

Spatial Variation in Creep Rate, Pre-1989

A space-time diagram showing creep rate as colored areas (Fig. 2) illustrates our early knowledge of approximate

creep rates from cultural features. The oldest feature dates from 1869, but only a few predate the 1930s (Lienkaemper and Galehouse, 1997). More frequent surveys, using an increased number of cultural features, were made across the fault beginning in the 1960s, and much better spatial coverage was realized by the late 1980s. These data showed distinctly higher rates of creep (~ 9 mm/yr) over a ~ 4 -km extent near the south end of the creeping HF (km 63–67), while the rest of the fault ranged from a low of 3–4 mm/yr in Oakland (km 20–27) to 4–6 mm/yr elsewhere. Excluding the south end high, the average creep rate was 4.6 mm/yr. The few surveyed rates available suggested that within error limits (± 0.1 – 0.2 mm/yr; Lienkaemper and Galehouse, 1997) average rates were consistent with the assumption of constancy over time when compared with rates from older offset features with larger estimated errors (± 0.2 – 0.8 mm/yr; Lienkaemper and Galehouse, 1997).

Effects of the 1989 Loma Prieta Earthquake: Static Stress Drop and Triggering

The M_w 6.9 Loma Prieta earthquake of 17 October 1989 was accompanied by profound changes in creep rates, particularly near the south end of the HF (km 63–67) where rates had been the highest (8–10 mm/yr), as shown by the coolest colors in Figure 2. The LPE essentially arrested creep in this

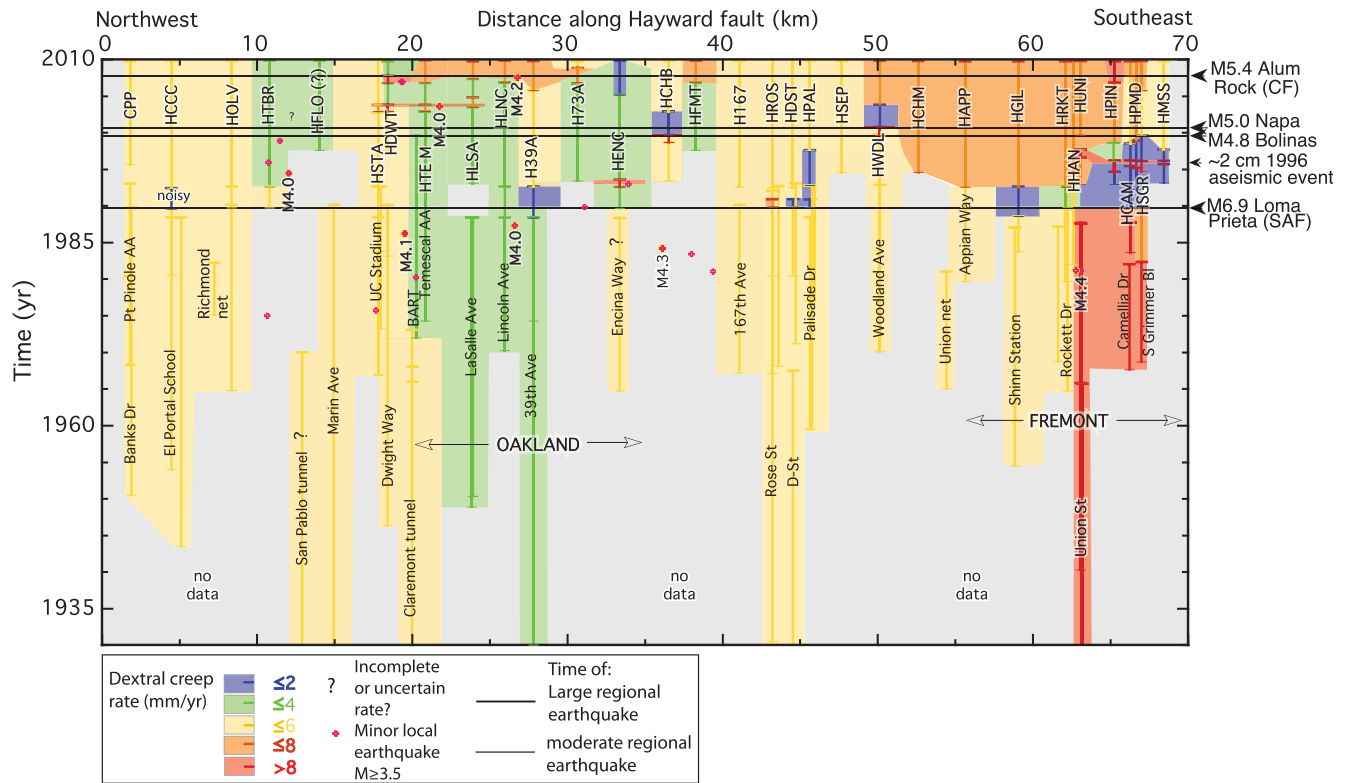


Figure 2. Variation of creep rate along the fault through time (data further described in [Spatial Variation in Creep Rate, Pre-1989](#) and [Effects of 1989 Loma Prieta Earthquake: Static Stress Drop and Triggering](#)). Increase in detail over the past 20 + years reflects increase in monitoring since the Loma Prieta earthquake. Temporal variations in creep suggest a variety of possible interactions with earthquakes: (1) minor events ($M \sim 4$) on the fault causing local stress changes, (2) moderate (M 4.5–5.5) regional events causing triggered slip, and (3) large ($M > 6$) regional events accompanied by significant regional stress changes.

area for about six years. This post-LPE pause in creep was consistent with simple elastic models predicting that a slight reversal of static shear stresses (~ 0.1 MPa), from dextral to sinistral, should be expected along the southernmost HF (Lienkaemper *et al.*, 1997, 2001). A large creep event (~ 20 mm) occurring on 9 February 1996 (see 1996 Fremont Creep Event for details) appeared to signal the end of the post-LPE pause. However, this event was followed unexpectedly by additional years of greatly reduced creep rate and slow recovery approaching pre-LPE rates.

In this paper, we attempt to develop an estimate of long-term, average creep rates that as much as possible removes the transient effects of the LPE (Fig. 3). Early estimates of Lienkaemper *et al.* (2001) suggested the creep response at the south end (km 63–67) was fully consistent with an elastic model of the LPE stress changes suggesting 3–5 cm of permanent, net sinistral slip retardation. However, the observed net retardation has been somewhat larger (4–9 cm, Fig. 4e), especially where pre-LPE creep rates had been highest. Over the past decade rates along km 63–67 of 6–10 mm/yr have begun to approximate pre-LPE rates (McFarland *et al.*, 2009). In contrast to a post-LPE net retardation in slip at the south end of HF, at two locations in the middle of the fault (H39A, km 27 and HPAL, km 45), the LPE apparently triggered dextral slip, apparently in response to shaking. This triggered slip was then followed by 3–6 years of negligible creep,

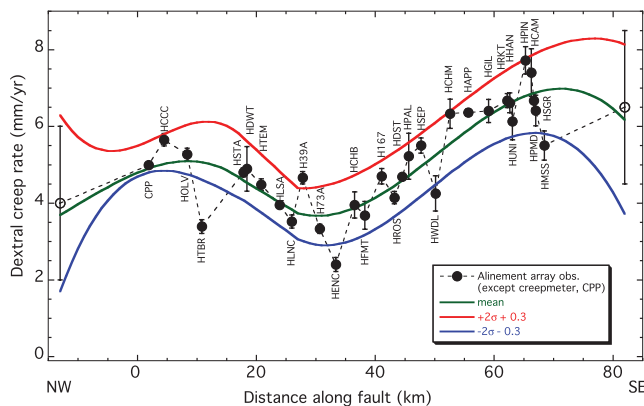


Figure 3. Variation of observed surface creep rate along the Hayward fault from alignment array surveys ($\pm 2\sigma$, McFarland *et al.*, 2009), except for creepmeter CPP at north end of fault (Bilham *et al.*, 2004). Locations of sites shown in Figure 1. These rates, revised with post-2001 data, are intended as input for updated estimates of depth of creep (see Simpson *et al.*, 2001; Lienkaemper *et al.*, 2001 for original estimates). Rates for arrays exhibiting the post-1989-LPE slowdown, exclude this slower period. Rates in Oakland include the 2007 slow-slip event. The mean rate (green curve) is derived by fitting two third-order polynomials. Open circles at kilometer -13 and kilometer 83 are assumed values (see Effects of 1989 Loma Prieta Earthquake: Static Stress Drop and Triggering). The curves for maximum (in red) and minimum (in blue) rate are from independently fitted polynomials from $\pm 2\sigma$ of each data point and include an additional 0.3 mm/yr of uncertainty.

finally ending in accelerated creep until reaching the background creep rate (McFarland *et al.*, 2009; $\text{\textcircled{E}}$ Fig. S5 in the electronic supplement to this paper has details on HPAL triggering). A similar pattern of changing creep rates has occurred at other locations on the HF as a result of shaking-induced triggering from regional events followed by a multi-year suspension of creep ending in accelerated creep (Fig. 2; at HCHB, km 36 from 52.7-km distance, M_w 4.8 earthquake near Bolinas, 18 August 1999; and at HWDL, km 50; from 88.1-km distance, M_w 5.0 earthquake near Napa on 3 September 2000). The closer M_w 5.4 Alum Rock 2007 earthquake northeast of San Jose, California, apparently caused some minor triggering, 1–4 mm above background rates, at five sites between Fremont and San Leandro, but was not followed by pronounced suspension of creep at any of these locations.

1996 Fremont Creep Event

The large creep event of 9 February 1996, although largely a consequence of the recovery from the 6-yr post-LPE pause in creep, is the largest (~ 2 cm) well-documented creep event yet measured on the fault (Fig. 4c). The overall timing of this large creep event is uncertain in detail, but it certainly propagated fairly rapidly, lasting only a few (~ 4) days. The event apparently began aseismically (shallowest background microseismicity in this section of HF tends to be 4–6 km deep, Waldhauser and Schaff, 2008). A strain event was recorded from 5 February to 9 February on three borehole strainmeters near Fremont at distances of 3.2, 4.8, and 8.8 km from the Hayward fault consistent with slip growing to 2 cm on a 3-km \times 1-km patch of fault at a depth of 4 km centered at km 65 (M. J. Johnston, written commun., 2010). Using our alignment array data, Kanu and Johnson (2011) have modeled this event as initiating at a depth somewhere within the range of ~ 4 –7.5 km depending on choice of method and the assumed values of rate-state parameters. A large water main broke and required repair near km 66 on 9 February; by that evening (6 p.m. local time; 0200 GMT) the fault showed abrupt onset of a creep event at creepmeter CFW (km 63.62, location in Fig. 1; $\text{\textcircled{E}}$ see Fig. S6 in the electronic supplement to this paper). The event ended at CFW in about two days. Alignment array data indicate that the event extended about 5 km from km 63.6 to km 68.5, although, at a lower speed (weeks to months) propagated 0.5 km farther north (km 63.1, HUNI, Fig. 2). It is interesting to compare this creep event with one of similar amplitude but longer extent in 2006 on the Superstition Hills fault in southern California that was documented in great detail by Wei *et al.* (2009). Using InSAR they were able to show that the displacement was skewed to the shallowest part (~ 2 km) of the depth range at which creep is thought to occur (~ 0 –4 km). Although the 5-km lateral extent of the HF creep event at the surface might suggest a limiting depth of ≤ 5 km, from their detailed models (boundary element and spring-slider) using our alignment array data Kanu and

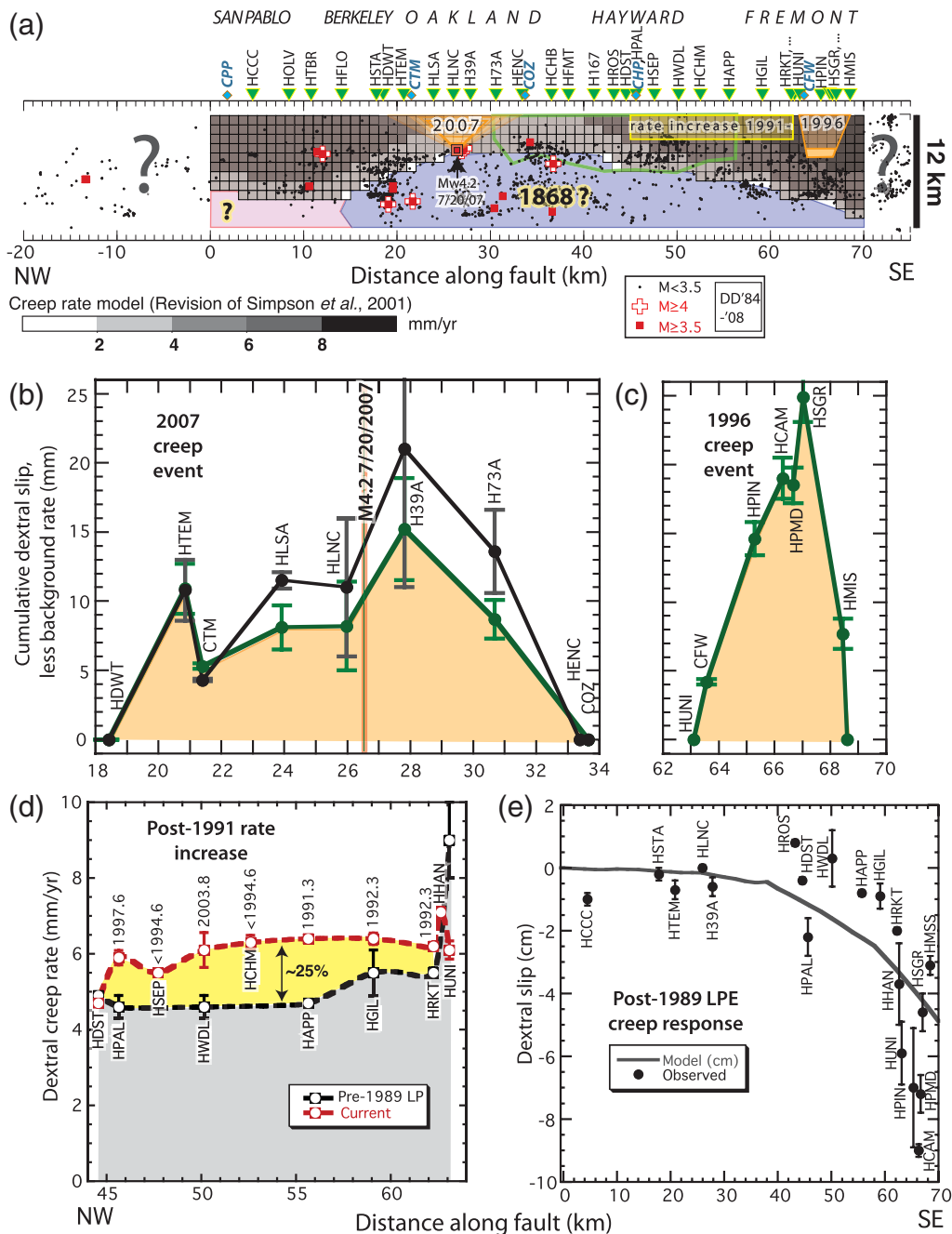


Figure 4. Estimated distribution of creep to locking depths, seismicity and creep transients along Hayward fault. (a) Cross-section showing estimated creep rates above locking depths using post-LPE rates shown in Figure 3; Orange patches indicate extent of 2007 and 1996 creep events; yellow patch, extent of ~25% increase in rate; red symbols, $M \geq 3.5$ earthquakes; black, $M < 3.5$, double-difference locations (1984–2008, Waldhauser and Schaff, 2008); Purple patch, inferred main locked area; pink, minor possible locking in north; green outline, extent of gabbro on both sides of fault; (b) slip (above background rate) associated with 2007 M_w 4.2 Oakland earthquake from multiple linear regression (in green) and using AFTER (in black; Boatwright *et al.*, 1989); (c) slip (above background rate) from creep event February 1996; (d), steplike increase in rate beginning in 1991 at HAPP, then propagating north and south; (e) observed net post-LPE change in slip from multiple linear regression using pre-LPE rates compared with results of elastic LPE rupture model of Simpson *et al.* (2001) shown in gray.

Johnson (2011) estimated the depth of this event may have been somewhat deeper, ~4–7.5 km. InSAR modeling by Lanari *et al.* (2007) shows good agreement with our alignment array data for the amount of surface creep in the 1996 event, but they could not constrain the depth range of the slip. To

estimate the equivalent moment released in the 1996 creep event, we use the average surface slip (13 mm) and assume slip tapers to zero at 5-km depth, thus yielding the moment equivalent (Hanks and Kanamori, 1979) to M_w 4.5 (± 0.1 , given uncertainties in depth distribution).

2007 Oakland Creep Event

An M_w 4.2 earthquake occurred 20 July 2007, in Oakland, near km 26.4 at a depth of 4.1 km (location shown in Figs. 1, 4a,b; 4.05 km depth estimate of J. Hardebeck, written commun., 2007, using 3D velocity model; 4.18 km depth estimate by double-difference method, Waldhauser and Schaff, 2008). Alinement array data over the following months and years indicate that this earthquake was followed by a slow ~ 10 – 20 mm surface creep event extending over at least 10 km (km 20.8–30.7), but no greater than 15 km (km 18.4–33.4, Fig. 4b). Although we made no immediate field inspection for surface slip, this creep event had reached creepmeter CTM (km 21.40) by 12 days postearthquake, indicating an average propagation speed of ~ 400 m/d or ~ 0.007 m/s. We used two methods to estimate the amount of creep above background rate at each alinement array and at CTM (Fig. 4b): (1) multiple linear regression (MLR) and (2) the program AFTER of Boatwright *et al.* (1989; Budding *et al.*, 1989). Because AFTER was calibrated for an earthquake having large afterslip (0.5–1 m) relative to a negligible background creep rate (~ 2 mm/yr), whereas we are analyzing a small signal (0.01–0.02 m) and larger creep rate (~ 4 mm/yr), we must exclude the background rate from our analysis of the postearthquake signal. Thus, we subtract the background creep rate from the data, so that AFTER only analyzes the excess signal of the creep event. The AFTER program provides estimates of event duration above background creep rate of 96 days (58–145 days, 99%-range) at CTM and 21 days (2–79 days, 65%-range) at HLSA (km 23.92), but determinations elsewhere are poor (see Fig. S1 in the electronic supplement to this paper). The MLR approach simply assumes that the latest measurements at each site are no longer affected by the 2007 transient, which except for H39A is a reasonable assumption but might slightly underestimate the amplitude of the transient signal. Multiple linear regression uses a dummy variable to compute the total transient as a step between all pre-2007 earthquake data and the final reading, excluding all data during the transient. In that AFTER may slightly overestimate the amplitude of the transient and MLR may underestimate it, we take the average of the two estimates as the best-available estimate.

To estimate limits on the equivalent moment release of this postseismic creep event, we approximate the depth of locking for this section of the fault at about 4 km (Simpson *et al.*, 2001; and this paper), and we assume that slip in this 2007 HF event was concentrated close to the surface as found by Wei *et al.* (2009) for the similar 2006 creep event on the Superstition Hills fault. Very shallow slip is also supported by a lack of detectable postseismic signal on regional borehole strainmeters (M. J. Johnston, written commun., 2010), although the southern part of this release occurred too slowly to be detectable. For a maximum estimate, we assume the 9.2 mm of average surface slip for this event (integrated from the average of MLR and AFTER estimates) is taken to decrease linearly to zero at a maximum depth of 4 km with

depth tapering to zero at the ends. These assumptions limit the seismic moment release of the 2007 creep event to the equivalent of a magnitude M_w 4.4 earthquake at most. For a minimum estimate, we assume a uniform 500 m deep patch with slip decreasing to zero at the base of it, which gives a minimum of only M_w 3.9. Hence, the postseismic release was probably similar to the seismic release (roughly M 4.2), but with considerable uncertainty.

It is interesting that the 2007 creep event, in contrast to the 1996 event farther south, began in response to a seismic event at the creeping-locked interface. In 1987 an earthquake of similar size (M_L 4.0, depth 4.6 km) occurred in the same location as the 2007 event, allowing that creep events associated with small earthquakes may not be unusual. Unfortunately, creep monitoring was then too sparse and infrequent to resolve a possible creep event following the 1987 earthquake. The next previous event with a catalog location within 1 km of the 2007 and 1987 events was an M_L 4.5 earthquake in 1937, suggesting that the size and frequency of such events is quite variable. Nevertheless, it seems likely that events such as these, to the degree that they encourage significant pulses of aseismic release above background rates, may be significant to assessing long-term creep rates along the Oakland section of the fault. Indeed, the site of the lowest long-term HF creep rate (HENC, km 33.39, 2.4 ± 0.1 mm/yr) shows pronounced stick-slip (i.e., eventful rather than steady slipping) behavior (McFarland *et al.*, 2009); its average creep rate is strongly influenced by the timing of a 14-mm creep event, which lasted about 8 months following an M_L 3.8 earthquake at 4.5-km depth that occurred in 1992 within a distance of ~ 0.5 km of the site.

1991-Onward Apparent Creep Rate Increase Near Union City

The Union City alinement array (HAPP, km 55.65) from 1979 to 1991 showed a steady creep rate of 4.7 ± 0.09 mm/yr, but beginning in early 1991 the rate became distinctly higher (6.4 ± 0.04 mm/yr, ~ 1991.3 –2009) (Fig. 4a,d; McFarland *et al.*, 2009). We recognize a general pattern of lateral expansion of increasing rates along the HF in the 1990s, both northward and southward of HAPP, with interruptions caused only by local transient effects at HWDL (triggered by the M 5.0 Napa earthquake in 2000, followed by a long pause in slip) and HPAL (triggered by the 1989 LPE, followed by a long pause in slip). Overall, the amount of increase in rate is about 25%. Because monitoring in this segment had been sparse before 1989, it is possible that our shorter-term pre-LPE rate at HAPP may be unrepresentative. Another early nearby measurement, USGS Union array (km 54.45; Prescott and Lisowski, 1983) indicated 5.3 ± 0.3 mm/yr (1965–1981), consistent with either the higher or lower rates within the uncertainty.

A possible explanation for the apparent rate increase is that post-LPE stress changes could be involved. However, only minor unclamping (≤ 0.2 bar) was expected for this

section of the fault (Lienkaemper *et al.*, 1997) and, given the compressive obliquity (Bilham and King, 1989) of most of this section of the fault, presumably any resulting decrease in friction would have been quickly eliminated by reloading. The expected minor reduction in creep from reduced shear stress post-LPE was mostly not realized in this section of the fault (Fig. 4e). Another possible explanation for the observed rates is that the greater accumulated stress late in the HF's seismic cycle may be sufficient to raise the aseismic release rates, perhaps by the expansion of the subsurface creeping area. In the absence of any certain explanation for this apparent increase in creep rates, for purposes of modeling the depth of creep, we regard the current rates as the best-available long-term rates for this section of the HF.

Spatial Variation in Creep Rate, Post-1989

A glance at the space–time diagram of creep rates along the fault (Fig. 2) shows that since the 1989 LPE there is much more heterogeneity, at least in our knowledge of creep rates as they change spatially over time, which needs to be considered when evaluating the meaning of long-term rates. Certainly the decade-long slowdown in creep in south Fremont (km 63–68; 1989–1999) had a significant impact on the local creep rates, which are only now resuming the pre-1989 rates. As just discussed, the apparent rate changes near Union City (km 46–62) since 1991 may be physically meaningful, or it may simply reflect the insufficiency of data in this area pre-1989. We assume that the post-1991 rates represent long-term rates.

The large creep event following the M_w 4.2 earthquake in Oakland in 2007 affects average creep rates over at least 10 km of the fault, but again our perceptions of the importance of this event are influenced by the greater amount of data available since 1989. In 1987, when an M 4.0 earthquake occurred at the same location as the M 4.2 in 2007, creep monitoring was sparse in Oakland, but available data do allow that a similar large creep event may have followed it (McFarland *et al.*, 2009). Consequently, it is probably best to consider the pulses of creep that may occur in Oakland intermittently as inherent to the long-term aseismic release process, even if not exactly a steady state process (nor strictly aseismic). Thus, we include the effects of such pulses of creep as part of the long-term averages used to estimate the depth of creeping along the fault. Including the 2007 creep event increases the average creep rate by only about 0.4 mm/yr. For purposes of modeling the depth of creep as described in the next section, this slight increase in rate only increases the calculated depth of creep in the Oakland area by about 0.5 km.

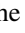
The long-term post-1989 average values obtained from alignment arrays (and creepmeter CPP) are shown in Figure 3 plotted with 2σ error. Polynomial curves were fitted to the mean values and to the upper and lower error limits (with an additional 0.3 mm/yr of uncertainty added to better acknowledge the existence of outliers from these curves).

The creep rates near the ends of HF (under San Pablo Bay and near its junction with central Calaveras fault [CF]) are poorly constrained, but we have estimated ranges for them as useful boundary constraints to the model. In San Pablo Bay, shallow microseismicity (Waldhauser and Schaff, 2008) continues aligned with the onland HF to near km –12 to –14, and its distribution appears consistent with creep continuing at levels similar to onshore rates. However, northward of \sim km –13, the seismicity bends toward and joins the south end of the Rodgers Creek fault (RCF), which has creep rates of only 0–2 mm/yr (McFarland *et al.*, 2009; $\text{\textcircled{E}}$ see Figs. S7–S10 on RCF in the electronic supplement to this paper). Similar arguments can be made that creep continues southward of our last surface observations on the HF (\sim km 69), and is collocated at depth with seismicity (and repeating earthquakes) that connects the HF to the central CF (Simpson *et al.*, 2004; Ponce *et al.*, 2004; Manaker *et al.*, 2005; Evans *et al.*, 2007), but is complexly distributed at the surface (Andrews *et al.*, 1993).

This curve of mean creep rate (Fig. 3) is our best current representation of the average, interseismic long-term creep rate on the Hayward fault and is intended as an update of the similar curve presented in Lienkaemper *et al.* (2001). There is one conspicuous difference between these two curves: the 2001 curve contains a small hump from km 30 to km 45, which was based almost entirely on two poorly determined rates from newly established arrays (HCHB, H167) representing only about six years of data. Now with 16 years of data, this hump, an artifact of insufficient data, entirely disappears. This has an important impact on modeling the depth of creep.

Depth Extent of Creep

Savage and Lisowski (1993) used a simple 2D geometry to estimate the depth extent of creep on the Hayward fault, driven by deep slip on the Hayward, Calaveras, and San Andreas faults. Simpson *et al.* (2001) elaborated on this calculation by including a more realistic 3D geometry for the faults and using slip at depth on all of the important regional faults, allowing variations in depth to locking to be estimated along the length of the Hayward fault. Updating the results of Simpson *et al.* (2001) by using the new average long-term creep rates, we attempt, as before, to explain the variation in surface creep rate along strike as variation in locking depth. To this purpose, the mean curve (Fig. 3; $\text{\textcircled{E}}$ see Table S1 in the electronic supplement to this paper) was used to interpolate average creep rates on to 1-km segments along the fault trace. A vertical fault surface was constructed of 1-km square dislocation patches extending to a depth of 12 km and laterally for \sim 100 km between the approximate junctions with the RCF and the central CF. A 12-km (\pm 2 km) depth is the depth of microseismicity along the HF (Working Group on California Earthquake Probabilities, 2003). Creep is driven in the model by screw dislocations below the 12-km depth under the HF, SAF, CF, and other major regional faults.

We have assumed that the 1×1 -km elements forming the Hayward part of the fault model are either locked or completely free to slip so as to reduce the shear stress acting on them to zero. The iterative method and other details of this modeling approach are explained in [Simpson *et al.* \(2001\)](#). The  electronic supplement to this paper contains a supplemental PDF file that allows the reader to step through a sequence showing the stepwise improvements in fit of the model to the creep rate data as the depth to creep is permitted to increase. We chose to start the modeling with a 2D approximation of depth of creep derived using the equations of [Savage and Lisowski \(1993\)](#). This converges after four iterations to the stable solution shown in [Figure 4a](#).

Our update of the [Simpson *et al.* \(2001\)](#) calculations ([Fig. 4a](#)) suggests that there may be a sizable area of relative locking (tinted light purple and labeled “1868?”) confined laterally between two zones of deeper-extending creep, plus a smaller area of locking below the northern creeping patch (tinted pink). We describe these areas as locked for simplicity, but they could also be areas of low, retarded creep, perhaps because they are pinned on one or more sides by fully locked asperities. In the updated calculation, the extent of the shallow locking area is larger than in the 2001 calculation, primarily because of the prior paucity of data between km 30 and km 45 as described previously. As a result, the new calculation is dominated by one large area of about 50-km length with shallow locking depths, where the earlier calculation showed two distinct areas of shallow locking depth.

Assuming that the HF was completely relaxed in 1868, if the moment currently stored in all of the inferred locked (retarded) areas of this updated calculation (from km 0 to km 70) were released, assuming uniform loading of 9 mm/yr since 1868, then the accumulated seismic moment would be the equivalent of an M_w 6.8 earthquake (M_w 6.9, if half of the energy stored in the surrounding creeping patches is released dynamically). Varying the depth of driving and assumed base of the locked area from $12 \text{ km} \times \pm 2 \text{ km}$ only changes the magnitude slightly (± 0.06). Alternatively, we allow coseismic rupture to penetrate downward below the seismogenic base of $12 \pm 2 \text{ km}$ as suggested by [King and Wesnousky \(2007\)](#) and [Hillers and Wesnousky \(2008\)](#). We assume that such a transitional region has been pinned during the interseismic period, such that strain accumulated there is then released coseismically. We find thus modeling the downward penetration of coseismic slip changes the expected magnitudes only negligibly (± 0.04). The estimated fraction of aseismic strain release (interseismic and postseismic) during such an earthquake cycle ranges from 26% to 78% compared with a non-creeping fault of the same rupture dimensions, depending largely on how much dynamic rupture release occurs in the creeping areas. We expect a substantial part of accumulated strain in the creeping patches to be released as afterslip ([B. T. Aagaard, J. J. Lienkaemper, and D. P. Schwartz, unpublished manuscript, 2011](#)). The mean recurrence interval (RI) for the past 12 southern HF earthquakes is $161 \pm 65 \text{ yr}$ ([Lienkaemper *et al.*, 2010](#)). For 161 yr of slip accumulation, the

results are essentially the same as previously mentioned. Thus, the fault is capable of repeating an M_w 6.8–6.9 earthquake at each mean RI. Because the 1868 earthquake was estimated at $\sim M_w$ 6.8 (6.5–7.0; [Bakun, 1999](#)), we suggest that it may have been a typical or characteristic earthquake caused primarily by rupture of the one large locked area.

Interestingly, the proposed large locked area includes the San Leandro gabbro (particularly where it forms both faces of the HF ([Fig. 4a](#); [Ponce *et al.*, 2003](#); [Graymer *et al.*, 2005](#); [Phelps *et al.*, 2008](#))). The gabbro exhibits the highest coefficient of friction (0.84) of the materials collected along the fault ([Morrow *et al.*, 2010](#)). The low creep rate section (km 25–40) includes where the fault has its most recent and complex fracturing through the gabbro (km 36–40) as evidenced by multiple splaying traces and < 100 -m extensional separation of intact gabbro at the main trace ([Lienkaemper, 2006](#)). The small extensional separation in gabbro is consistent with the main fault trace at this location having formed in the latest Pleistocene ($< 100 \text{ ka}$). This location, the San Leandro salient (km 36–40), is also the most misaligned (by 0.7 km) from the overall trend of the HF ([Lienkaemper *et al.*, 1991](#)), and thus is a reasonable place to expect greater resistance to creep. The main trace through the San Leandro salient apparently has not experienced enough slip to develop the same level of maturity or smoothness as the rest of the fault, and thus the greater friction likely contributes to the locally more pronounced stick-slip behavior (e.g., at HENC, HCHB especially; [McFarland *et al.*, 2009](#)).

That the strongest asperity of the fault may be so localized (km 36–40) supports the idea that the large locked patch inferred from our depth to locking estimates may be pinned by small stuck areas. Such stuck areas could retard aseismic slip elsewhere on the locked patch to near zero, but it is possible most of the nominally locked area is relatively weak and smaller than a noncreeping Hayward fault would be. The fault as a whole appears to exhibit low effective friction (~ 0.1 – 0.3 ; [Reasenber and Simpson, 1997](#)), thus much weaker than the highest friction (~ 0.8 ; [Morrow *et al.*, 2010](#)), suggesting a possible difference in strength of roughly a factor of 4. A hypothetical noncreeping Hayward fault could have locking areas capable of failure over lengths of $\sim 96 \text{ km}$, producing significantly larger ruptures $M \sim 7.2$ ([Hanks and Bakun, 2002, 2008](#)) and average slip of $\sim 2.2 \text{ m}$ ([Wesnousky, 2008](#)). Thus, a noncreeping HF could thus sustain longer recurrence intervals, for example, $\sim 240 \text{ yr}$ on average ($2.2 \text{ m}/0.009 \text{ m/yr}$), than the actual observed mean RI of $\sim 160 \text{ yr}$ for this creeping fault. Hence, we suggest that because the stuck area is relatively small and weak compared with a more generic fault with no creep, this tends to make recurrence intervals relatively short and regular.

Discussion

At only 161 yr, the mean RI on the southern HF, as averaged over the past two millennia from paleoseismic studies near km 60, is relatively short compared with recurrence

estimates for other major faults in the San Francisco Bay region (Dawson *et al.*, 2008; Working Group on California Earthquake Probabilities, 2008; Lienkaemper *et al.*, 2010). For example, a site on the northern HF near km 10 (RI = ~ 330 yr; Hayward Fault Paleoequake Group, 1999; Dawson *et al.*, 2008) and the RCF (RI = ~ 305 yr; Dawson *et al.*, 2008) appear to have earthquakes roughly half as frequently. We suggest that a large locked patch on the Hayward fault (purple patch in Fig. 4a) may behave as a mechanical capacitor controlling both earthquake size and recurrence interval. The RCF in contrast, although somewhat shorter (~ 65 km) than the HF, is almost entirely locked and fails at longer intervals.

The timing constraints for the most recent paleoearthquakes on the northern HF and RCF allow a possible coincidence with the penultimate southern HF earthquake. Previous interpretations have generally treated the connection between HF and RCF simply as an ~ 5 – 6 km right-stepover structure, and both historical rupture data (Wesnousky, 2008) and dynamic modeling (Harris and Day, 1993) suggest that ruptures are unlikely to jump 5-km or larger stepovers, including the HF-RCF junction specifically. However, new location data for microseismicity in the stepover area appear to suggest that the HF links to RCF by an abrupt, but throughgoing releasing bend (Fig. 1 inset; Waldhauser and Schaff, 2008; ⑤ see Figs. S7–S10 on RCF in the electronic supplement to this paper). Even though the possible presence of a bend connecting the HF to the RCF might somewhat increase the probability of throughgoing ruptures ($M_w \sim 7.1$ – 7.25 ; Working Group on California Earthquake Probabilities, 2003), the presence of a large, deeply creeping area (~ 9 km deep; Fig. 4a) over the northern third of the HF would tend to reduce the likelihood of ruptures continuing from the RCF onto the HF (Harris *et al.*, 2008). Likewise ruptures starting in the southern or central HF would tend to slow and stop when encountering such a large area of velocity-strengthening region, thus lessening the likelihood of connection to the RCF. Despite the zone of deep creep on the northern HF inferred by this and other studies (Bürgmann *et al.*, 2000; Funning *et al.*, 2007), the Mira Vista trench site at km 10.05 (Hayward Fault Paleoequake Group, 1999) shows evidence for multiple if less frequent paleoruptures on the northern Hayward fault. One possible explanation for the occurrence of such ruptures is that they may result entirely from rapidly accumulated afterslip associated with the largest southern HF ruptures and may include rupture of the smaller, northern locked patch (pink area in Fig. 4a). Although considered less likely, some of the Mira Vista ruptures may have initiated on the RCF.

Although one might expect fault interactions to have major impact on either advancing or retarding large earthquakes on the HF, the largest historical earthquake in the region apparently did not. The great 1906 earthquake ($M 7.8$) on the nearby San Andreas fault appears to have had modest impact on HF creep rates (Lienkaemper and Galehouse, 1997), and modeling of the post-1906 creep response on the

HF (Schmidt and Bürgmann, 2008) suggests a relatively short-lived (~ 20 – 30 yr; ~ 0.3 MPa) reduction in the accumulated strain. Therefore, variations in earthquake size and frequency on the HF may depend primarily on processes within the HF alone, with the possible major exception of a much larger event cascading from the RCF.

Summary and Conclusions

Improved knowledge of both spatial and temporal variations in the HF creep rate gained over the past 20 years since the LPE gives us greater insight into the process of strain release along the fault. The two most substantial transient changes in rate occurred as sizable (1–2 cm) creep events that propagated over two multi-kilometer-long sections of the fault, in 1996 in Fremont and in 2007 in Oakland. The 1996 creep event was purely aseismic and appears to be associated with the resumption of loading following a six-year arrest of creep caused by stress reduction induced by the LPE. In contrast, an $M_w 4.2$ earthquake in Oakland in 2007 at the creeping-locked interface initiated a slow 12-day bilateral propagation of a creep event. This event lasted 20 to 100 days northward of the epicenter, but continued for up to two years to the south of it. This 2007 event may be representative of a somewhat irregular pattern of creep release in the Oakland section of the HF that accounts for significant local strain release, estimated as contributing $\sim 10\%$ of the local long-term interseismic creep rate. An apparent $\sim 25\%$ increase in creep rates since 1991 centered near Union City (km 46–62) is of unknown origin and may be caused by an expanding creep area at depth or, alternatively, may be an artifact of the sparser pre-LPE data observations, which may not have adequately captured the long-term rates.

Of greatest impact to our understanding the depth of creep is simply the greater amount of long-term data now available, in particular for a middle part of the fault where creep had been poorly sampled in the past (km 35–45). Here the lowest creep rates of the HF appear to be associated with the fault's largest geometric irregularity (the San Leandro salient) and the material exhibiting the highest coefficient of friction (the San Leandro gabbro). An update of the depth of creep estimates of Simpson *et al.* (2001) using the new average long-term creep rates suggests that there is a single large area of retarded slip on the fault approximately centered below the San Leandro salient, lying between two regions in which creep extends to greater depths (one in south Fremont and another extending from north Berkeley to San Pablo Bay). The size of this large area of retarded slip, assuming a 9-mm/yr loading rate on the fault, is consistent with $M_w 6.8$ (± 0.2) ruptures occurring each 161 ± 65 yr (mean RI; Lienkaemper *et al.*, 2010). We suggest that the size and strength of this locked area tend to control ruptures both in their magnitude and recurrence interval.

Data and Resources

All data used in this paper came from published sources listed in the references and online resources for Hayward fault creep data at the following links (last accessed September 2011): alignment array data (1979–2010), <http://pubs.usgs.gov/of/1997/of97-690/>; creepmeter data, <http://cires.colorado.edu/~bilham/creepmeter.file/creepmeters.htm>; earlier creep rate data, <http://pubs.usgs.gov/of/1997/of97-690/>.

Acknowledgments

The USGS National Earthquake Hazard Reduction Program (SIR: 9939-0KR02; external: G10AC00139, SFSU and G10AC00161, University of Colorado) funded the investigation. We thank the many student surveyors from San Francisco State University whose diligent efforts since 1979, following the rigorous procedures developed by Jon Galehouse, have made this long-term creep monitoring effort possible. Malcolm Johnston kindly provided unpublished borehole strainmeter data and models for the 1996 and 2007 creep events. Roland Bürgmann gave useful suggestions on the preliminary manuscript. We thank reviewers Malcolm Johnston, Suzanne Hecker, Pascal Bernard, and an anonymous reviewer for their thoughtful reviews that greatly improved the manuscript.

References

- Andrews, D. J., D. H. Oppenheimer, and J. J. Lienkaemper (1993). The Mission link between the Hayward and Calaveras faults, *J. Geophys. Res.* **98**, 12,083–12,095.
- Bakun, W. H. (1999). Seismic activity of the San Francisco Bay region, *Bull. Seismol. Soc. Am.* **89**, 764–784.
- Bilham, R., and G. King (1989). Slip distribution on oblique segments of the San Andreas fault, California: Observations and theory, *U.S. Geol. Surv. Open-File Rept.* 89-315, 80–93.
- Bilham, R., N. Suszek, and S. Pinkney (2004). California creepmeters, *Seismol. Res. Lett.* **75**, 481–492.
- Blanchard, F. B., and G. L. Laverty (1966). Displacements in the Claremont water tunnel at the intersection with the Hayward fault, *Bull. Seismol. Soc. Am.* **56**, 291–294.
- Boatwright, J., K. E. Budding, and R. V. Sharp (1989). Inverting measurements of surface slip on the Superstition Hills fault, *Bull. Seismol. Soc. Am.* **79**, 411–423.
- Bonilla, M. G. (1966). Deformation of railroad tracks by slippage on the Hayward fault in the Niles district of Fremont, California, *Bull. Seismol. Soc. Am.* **56**, 281–290.
- Budding, K. E., J. Boatwright, R. V. Sharp, and J. L. Saxton (1989). Compilation and analysis of displacement measurements obtained on the Superstition Hills fault zone and nearby faults in Imperial Valley, California, following the earthquakes of November 24, 1987, *U.S. Geol. Surv. Open File Rept.* 89-140, 90 pp.
- Bürgmann, R., D. Schmidt, R. M. Nadeau, M. d'Alessio, E. Fielding, D. Manaker, T. V. McEvilly, and M. H. Murray (2000). Earthquake potential along the northern Hayward fault, *Science* **289**, 1178–1182.
- Cluff, L. S., and K. V. Steinbrugge (1966). Hayward fault slippage in the Irvington–Niles districts of Fremont, California, *Bull. Seismol. Soc. Am.* **56**, 257–279.
- Dawson, T. E., R. J. Weldon II, and G. P. Biasi (2008). Appendix B: Recurrence interval and event age data for type A faults, *U.S. Geol. Surv. Open-File Rept.* 2007-1437B, 40 pp., appendix to *U.S. Geol. Surv. Open-File Rept.* 2007-1437 (<http://pubs.usgs.gov/of/2007/1437/b/of2007-1437b.pdf>, last accessed September 2011).
- Evans, E., R. Bürgmann, and R. M. Nadeau (2007). Linking faults: Subsurface creep on a contiguous fault structure connecting the Hayward and Calaveras faults, *Eos Trans. AGU* **88**, Fall Meet. Suppl., Abstract S21A-0240.
- Funning, G. J., R. Bürgmann, A. Ferretti, and F. Novali (2007). Asperities on the Hayward fault resolved by PS-InSAR, GPS and boundary element modeling, *Eos Trans. AGU* **88**, no. 52, Fall Meet. Suppl., Abstract S23C-04.
- Graymer, R. W., D. A. Ponce, R. C. Jachens, R. W. Simpson, G. A. Phelps, and C. M. Wentworth (2005). Three-dimensional geologic map of the Hayward fault, northern California: Correlation of rock units with variations in seismicity, creep rate, and fault dip, *Geology* **33**, 521–524.
- Hanks, T. C., and W. H. Bakun (2002). A bilinear source-scaling model for M-log A observations of continental earthquakes, *Bull. Seismol. Soc. Am.* **92**, 1841–1846.
- Hanks, T. C., and W. H. Bakun (2008). M-log A observations for recent large earthquakes, *Bull. Seismol. Soc. Am.* **98**, 490–494.
- Hanks, T. C., and H. Kanamori (1979). A moment-magnitude scale, *J. Geophys. Res.* **84**, 2348–2350.
- Harris, R. A., M. Barall, and R. W. Simpson (2008). Preliminary 3D spontaneous rupture models of the Hayward fault, *Seismol. Res. Lett.* **79**, 342.
- Harris, R. A., and S. M. Day (1993). Dynamics of fault interaction: Parallel strike-slip faults, *J. Geophys. Res.* **98**, 4461–4472.
- Hayward Fault Paleoearthquake Group (1999). Timing of paleoearthquakes on the northern Hayward fault—Preliminary evidence in El Cerrito, California, *U.S. Geol. Surv. Open-File Rept.* 99-318, 94 pp. (<http://geopubs.wr.usgs.gov/open-file/of99-318/>, last accessed September 2011).
- Hillers, G., and S. G. Wesnousky (2008). Scaling relations of strike-slip earthquakes with different slip-rate-dependent properties at depth, *Bull. Seismol. Soc. Am.* **98**, 1085–1101.
- Kanu, C., and K. Johnson (2011). Arrest and recovery of frictional creep on the southern Hayward fault triggered by the 1989 Loma Prieta, California, earthquake and implications for future earthquakes, *J. Geophys. Res.* **116**, B04403, 22 pp., doi 10.1029/2010JB007927.
- King, G. C. P., and S. G. Wesnousky (2007). Scaling of fault parameters for continental strike-slip earthquakes, *Bull. Seismol. Soc. Am.* **97**, 1833–1840.
- Lanari, R., F. Casu, M. Manzo, and P. Lundgren (2007). Application of the SBAS-DInSAR technique to fault creep: A case study of the Hayward fault, California, *Rem. Sens. Environ.* **109**, 20–28, doi 10.1016/j.rse.2006.12.003.
- Lawson, A. C., (1908, reprinted 1969). The Earthquake of 1868, in *The California Earthquake of April 18, 1906, Report of the State Earthquake Investigation Commission* v. I, A. C. Lawson, chairman, Carnegie Institution of Washington, Washington, D.C., 434–438.
- Lienkaemper, J. J. (1992). Map of recently active traces of the Hayward fault, Alameda and Contra Costa counties, California, *U.S. Geol. Surv. Misc. Field Studies Map.* MF-2196, 13 pp. (1 sheet).
- Lienkaemper, J. J. (2006). Digital database of recently active traces of the Hayward fault, California, *U.S. Geol. Surv. Data Series.* DS-177, 20 pp. (<http://pubs.usgs.gov/ds/2006/177/>, last accessed September 2011).
- Lienkaemper, J. J., and G. Borchardt (1996). Holocene slip rate of the Hayward fault at Union City, California, *J. Geophys. Res.* **101**, 6099–6108.
- Lienkaemper, J. J., G. Borchardt, and M. Lisowski (1991). Historic creep rate and potential for seismic slip along the Hayward fault, California, *J. Geophys. Res.* **96**, 18,261–18,283.
- Lienkaemper, J. J., and J. S. Galehouse (1997). Revised long-term creep rates on the Hayward fault, Alameda and Contra Costa counties, California, *U.S. Geol. Surv. Open-File Rept.* 97-690, 18 pp. (<http://pubs.usgs.gov/of/1997/of97-690/>, last accessed November 2011).
- Lienkaemper, J. J., J. S. Galehouse, and R. W. Simpson (1997). Creep response of the Hayward fault to stress changes caused by the Loma Prieta earthquake, *Science* **276**, 2014–2016.
- Lienkaemper, J. J., J. S. Galehouse, and R. W. Simpson (2001). Long-term monitoring of creep rate along the Hayward fault and evidence for a lasting creep response to 1989 Loma Prieta earthquake, *Geophys. Res. Lett.* **28**, 2265–2268.

- Lienkaemper, J. J., P. L. Williams, and T. P. Guilderson (2010). Evidence for a twelfth large earthquake on the southern Hayward fault in the past 1900 years, *Bull. Seismol. Soc. Am.* **100**, doi [10.1785/0120090129](https://doi.org/10.1785/0120090129).
- Manaker, D. M., A. J. Michael, and R. Bürgmann (2005). Subsurface structure and kinematics of the Calaveras–Hayward fault stepover from three-dimensional V_p and seismicity, San Francisco Bay Region, California, *Bull. Seismol. Soc. Am.* **95**, 446–470, doi [10.1785/0120020202](https://doi.org/10.1785/0120020202).
- McFarland, F. S., J. J. Lienkaemper, and S. J. Caskey (2009). Data from Theodolite measurements of creep rates on San Francisco Bay region faults, California: 1979–2009, *U.S. Geol. Surv. Open-File Rept. 09-1119*, 17.
- Morrow, C. A., D. E. Moore, and D. A. Lockner (2010). Dependence of frictional strength on compositional variations of Hayward fault rock gouges, *U.S. Geol. Surv. Open-File Rept. 2010-1184*, 22 pp.
- Nason, R. D. (1971). Investigation of fault slippage in northern and central California, *Ph.D. Thesis*, University of California, San Diego, California, 231 pp.
- Phelps, G. A., R. W. Graymer, R. C. Jachens, D. A. Ponce, R. W. Simpson, and C. M. Wentworth (2008). Three-dimensional geologic map of the Hayward fault zone, San Francisco Bay region, California, *U.S. Geol. Surv. Scientific Invest. Map 3045*, 35 pp.
- Ponce, D. A., T. G. Hildenbrand, and R. C. Jachens (2003). Gravity and magnetic expression of the San Leandro gabbro with implications for the geometry and evolution of the Hayward fault zone, northern California, *Bull. Seismol. Soc. Am.* **93**, 14–26.
- Ponce, D. A., R. W. Simpson, R. W. Graymer, and R. C. Jachens (2004). Gravity, magnetic, and high-precision relocated seismicity profiles suggest a connection between the Hayward and Calaveras faults, northern California, *G³* **5**, no. 7, 39 pp.
- Prescott, W. H., and M. Lisowski (1983). Strain accumulation along the San Andreas fault system east of San Francisco Bay, California, *Tectonophysics* **97**, 41–56.
- Radbruch, D. H., and B. J. Lennert (1966). Damage to culvert under Memorial Stadium, University of California, Berkeley, caused by slippage in the Hayward fault zone, *Bull. Seismol. Soc. Am.* **56**, 295–304.
- Reasenber, P. A., and R. W. Simpson (1997). Response of regional seismicity to the static stress change produced by the Loma Prieta earthquake, *U.S. Geol. Surv. Prof. Paper 1550-D*, 49–71.
- Savage, J. C., and M. Lisowski (1993). Inferred depth of creep on the Hayward fault, central California, *J. Geophys. Res.* **98**, 787–793.
- Schmidt, D. A., and R. Bürgmann (2008). Predicted reversal and recovery of surface creep on the Hayward fault following the 1906 San Francisco earthquake, *Geophys. Res. Lett.* **35**, L19305, 5 pp., doi [10.1029/2008GL035270](https://doi.org/10.1029/2008GL035270).
- Schulz, S. S. (1989). Catalog of creepmeter measurements in California from 1966 through 1988, *U.S. Geol. Surv. Open-File Rept. 89-650*, 193 pp.
- Simpson, R. W., R. W. Graymer, R. C. Jachens, D. A. Ponce, and C. M. Wentworth (2004). Cross-sections and maps showing double-difference relocated earthquakes from 1984–2000 along the Hayward and Calaveras faults, California, *U.S. Geol. Surv. Open-File Rept. 04-1083* (<http://pubs.usgs.gov/of/2004/1083/>, last accessed September 2011).
- Simpson, R. W., J. J. Lienkaemper, and J. S. Galehouse (2001). Variations in creep rate along the Hayward fault, California, interpreted as changes in depth of creep, *Geophys. Res. Lett.* **28**, 2269–2272.
- U.S. Geological Survey and California Geological Survey (2006). Quaternary fault and fold database for the United States, *U.S. Geol. Surv. and California Geol. Surv.* (<http://earthquake.usgs.gov/regional/qfaults/>, last accessed September 2011).
- Waldhauser, F., and D. P. Schaff (2008). Large-scale relocation of two decades of northern California seismicity using cross-correlation and double-difference methods, *J. Geophys. Res.* **113**, B08311, doi [10.1029/2007JB005479](https://doi.org/10.1029/2007JB005479) (v200812.1.1, <http://www.ldeo.columbia.edu/~felixw/DDcatalogs/index.html>, last accessed September 2011).
- Wei, M., D. Sandwell, and Y. Fialko (2009). A silent M_w 4.7 slip event of October 2006 on the Superstition Hills fault, southern California, *J. Geophys. Res.* **114**, B07402, 15 pp., doi [10.1029/2008JB006135](https://doi.org/10.1029/2008JB006135).
- Wesnousky, S. G. (2008). Displacement and geometrical characteristics of earthquake surface ruptures: Issues and implications for seismic-hazard analysis and the process of earthquake rupture, *Bull. Seismol. Soc. Am.* **98**, 1609–1632.
- Working Group on California Earthquake Probabilities (2003). Earthquake probabilities in the San Francisco Bay Region: 2000–2030: *U.S. Geol. Surv. Open File Rept. 03-214*, 235 pp. (<http://pubs.usgs.gov/of/2003/of03-214/>, last accessed September 2011).
- Working Group on California Earthquake Probabilities, 2007 (2008). The Uniform California Earthquake Rupture Forecast, Version 2 (UCERF 2), *U.S. Geol. Surv. Open File Rept. 2007-1437*, Version 1.1. (<http://pubs.usgs.gov/of/2007/1437/>, last accessed September 2011).
- U.S. Geological Survey
MS 977, 345 Middlefield Rd.
Menlo Park, California 94025
jlienka@usgs.gov
(J.J.L., R.W.S., D.A.P., J.J.B.)
- Dept. of Geosciences
San Francisco State University
San Francisco, California 94132
(F.S.M., S.J.C.)
- Dept. Geological Sciences
University of Colorado
2200 Colorado Ave.
Boulder, Colorado 80309
(R.G.B.)